

Formation of Ethane Clathrate Hydrate in Ultrahigh Vacuum by Thermal Annealing

Bijesh K. Malla, Gaurav Vishwakarma, Soham Chowdhury, Premkumar Selvarajan, and Thalappil Pradeep*



Cite This: *J. Phys. Chem. C* 2022, 126, 17983–17989



Read Online

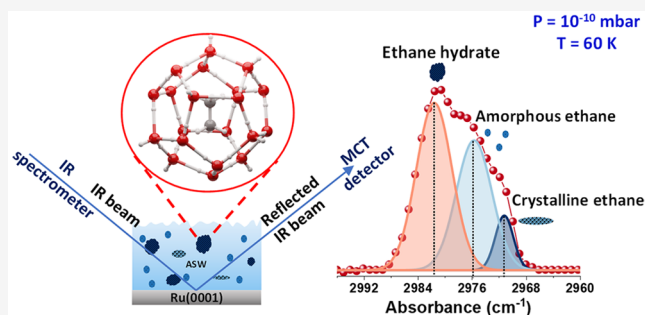
ACCESS |

Metrics & More

Article Recommendations

Supporting Information

ABSTRACT: The existence of many molecules in the form of clathrate hydrates (CHs) in ultrahigh vacuum (UHV) and cryogenic conditions has not been explored adequately. In the present study, a detailed investigation by reflection absorption infrared spectroscopy confirmed that the three phases of ethane, i.e., amorphous, crystalline, and CH, coexist in a vapor-deposited ethane–water mixture at 60 K in UHV. Experiments were conducted with vapor-deposited ice films at 10 K, which were annealed to 60 K for tens of hours, and the IR spectral evolution was monitored systematically. Upon maintaining the system at 60 K, three phases of ethane were seen to coexist, but a gradual increase in the hydrate phase was noticed. The evolution of ethane CH from the amorphous ethane–water ice mixture was observed for the very first time in UHV under cryogenic conditions. The formation of the CH was further confirmed by temperature-programmed desorption (TPD) mass spectrometry. Quantum chemical calculation suggested the formation of 5¹²6² cage of structure I CH in the ice matrix. The formation of ethane CH in a thin ice film at such a low temperature under UHV suggests its existence in the cometary environment.



INTRODUCTION

Clathrate hydrates (CHs), cages of water molecules formed by hydrogen bonding, are known since 1810.¹ These crystalline inclusion compounds are commonly known to have three types of structures: structure I (sI, cubic $Pm\bar{3}n$), structure II (sII, cubic $Fd\bar{3}m$), and structure H (sH, hexagonal $P6/mmm$).² CHs are considered as potential sources of energy and are likely to play an essential role in some of the planet's significant environmental challenges,³ such as energy storage and transportation,⁴ CO₂ sequestration,⁵ and water desalination.⁶ These molecular solids are found on the ocean floor and in the permafrost region of the earth. It is also believed to be present in the solar system, like the martian surface,^{7,8} titan surface,⁹ and icy moons.¹⁰ The capability of forming these structures depends mainly upon the pressure and temperature conditions.¹¹ Macroscopic deposits of hydrates generally occur at higher pressures,¹² typically greater than 25 atm for methane.^{13,14} CHs are also known to exist in vacuum, even under cryogenic conditions.^{15–17} In our previous study,¹⁸ we have shown the existence of sI methane hydrate at 30 K and 10^{−10} mbar. Upon annealing the methane–water ice mixture deposited at 10 to 30 K for an extended period, methane CH was formed. Such pressure and temperature conditions resemble the interstellar medium (ISM).

While X-ray diffraction, differential scanning calorimetry, and Raman spectroscopy were typically used to examine CHs

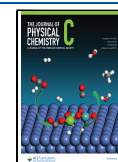
in bulk,^{19,20} their existence in UHV is typically studied by infrared spectroscopy, temperature-programmed desorption mass spectrometry, and reflection high-energy electron diffraction²¹ performed on a thin film.^{22–24} Recently, Bauer et al. showed the detection of methane and carbon dioxide CH in a high vacuum by in situ synchrotron X-ray diffraction.¹⁷ Cryo-electron microscopy has been used to examine the different crystalline states of water but has not been used yet for CH studies.²⁵

Hydrates formed at the cryogenic temperature in UHV have several consequences. Dissociation of these hydrates could lead to the formation of crystalline ice. In UHV, CHs of acetone and formaldehyde were converted to cubic and hexagonal ices upon dissociation of the hydrate cages.^{21,26} Also, it has been observed that ice XVI can be created by subjecting neon hydrate to pumping in a vacuum.²⁷ Physical properties such as density and refractive index of such ice forms may have important relevance for planetary objects. Similar could be the implication of chemistry of molecules confined in cages in the

Received: September 1, 2022

Revised: October 3, 2022

Published: October 14, 2022



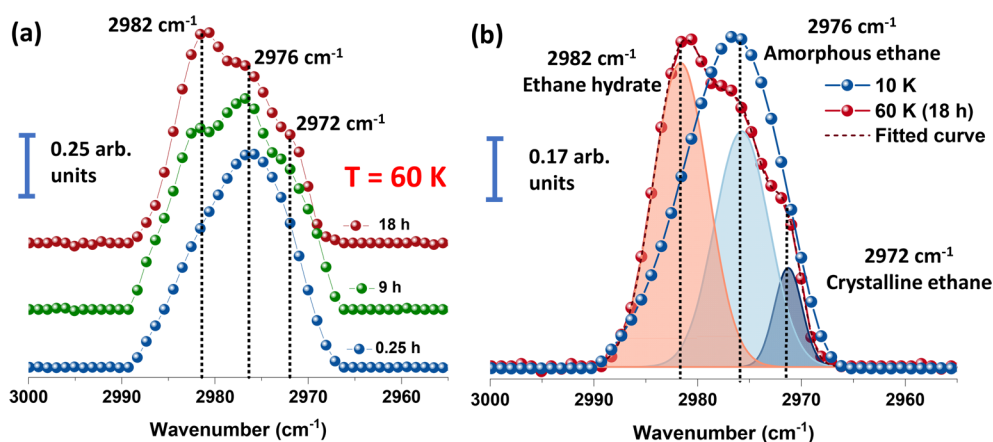


Figure 1. CH formation of ethane was studied by RAIR spectroscopy. (a) Normalized time-dependent RAIR spectra of 300 ML ethane/H₂O (1:1) ice mixture at 60 K in C–H antisymmetric stretching region. (b) A comparison of the normalized RAIR spectra of 300 ML ethane/H₂O (1:1) mixed ice at 10 and 60 K (after 18 h). The spectrum labeled as 60 K (18 h) was deconvoluted to three components, shown in orange (2982 cm⁻¹), light blue (2976 cm⁻¹), and dark blue (2972 cm⁻¹) shades. For these experiments, ethane and water vapor were codeposited on Ru(0001) at 10 K then the resulting ice mixture was annealed to 60 K at a ramping rate of 2 K min⁻¹.

astrochemical environment.²⁸ The existence of methane hydrate could be likely in such an environment. In the ISM environment, more than two hundred and 70 molecules, including water, have been detected in various temperature and pressure regions, suggesting the existence of hydrates in various astrophysical environments.²⁹ Chemical processes in these hydrates may lead to relevant cometary and prebiotic science.^{30,31} Expanding the exploration of CH to other molecules may be rewarding from this background.

Mixed hydrates of ethane and oxirane (commonly referred to as ethylene oxide) are known to exist in a high vacuum (10⁻⁷ mbar) at 90 K,³² however, to the best of our knowledge, pure ethane CH in UHV has not been reported yet. In the previous work of Richardson et al.,³² ethane-oxirane mixed hydrates nucleated over oxirane hydrate upon subsequent deposition of the ethane-oxirane-water mixture at 120 K in high vacuum (10⁻⁷ mbar). The presence of oxirane in the ice mixture helped to induce the nucleation of ethane-oxirane mixed hydrate. Several attempts were unsuccessful to prepare pure ethane hydrate in high vacuum. So, no high vacuum method was developed for the direct formation of ethane CH from ethane–water ice mixture. In this work, we present the formation of pure ethane CH from vapor-deposited ethane–water ice mixtures. This study is carried out at a lower pressure of 10⁻¹⁰ mbar and at a lower temperature of 60 K than all the previous related studies. Our results of ethane hydrate from binary mixtures of ethane and water may have direct relevance to the cometary environment, where ethane and water are present approximately in the ratio of 100:0.4.^{33,34}

EXPERIMENTAL SECTION

All the experiments were carried out in an ultrahigh vacuum instrument (with a base pressure of ~10⁻¹⁰ mbar), discussed in detail elsewhere.³⁵ The instrument is made of stainless steel, and it has three UHV chambers (namely ionization, octupole, and scattering chamber) equipped with low energy ion scattering (LEIS), temperature-programmed desorption (TPD) mass spectrometry, Cs⁺ ion-based secondary ion mass spectrometry (SIMS), and reflection absorption infrared spectroscopy (RAIRS). The base pressure of the vacuum chambers is maintained by six turbomolecular pumps, further backed by several oil-free diaphragm pumps. The vacuum of

the chambers is monitored by a Bayard-Alpert gauge, controlled by a MaxiGauge vacuum gauge controller (Pfeiffer, Model TPG 256 A).

We used a highly polished Ru(0001) single crystal as a substrate to create thin ice films. The substrate is mounted on a copper holder, and it is attached to the tip of the helium cryostat (Cold Edge technology), which can maintain a temperature as low as 8 K. The substrate can be heated up to 1000 K by a resistive heater (25 Ω), controlled by a temperature controller (lakeshore 336). A K-type thermocouple sensor is used to measure the substrate temperature with an accuracy of 0.5 K. Repeated heating to 400 K before each vapor deposition experiment ensured surface cleanliness, adequate for the present experiments. It is worth noting that the surface has no effect in this study due to the multilayer deposition.

Millipore water (H₂O of 18.2 MΩ resistivity) was taken in a vacuum-sealed test tube (with a glass-to-metal seal) and was further purified by several freeze–pump–thaw cycles. Ethane (Akkaran gas and energy, 99.9%) was directly connected to the sample line through a needle valve. Ethane and water were connected to the UHV chamber through two different sample inlet lines. The deposition of two samples was controlled through all metal leak valves, and monolayer coverage was calculated assuming that 1.33 × 10⁻⁶ mbar s = 1 ML, which was estimated to contain ~1.1 × 10¹⁵ molecules cm⁻².³⁶ For 300 ML of 1:1 mixed ethane and water deposition, the chamber was backfilled at a total pressure of 5 × 10⁻⁷ mbar where ethane pressure was 2.5 × 10⁻⁷ mbar, and water pressure was 2.5 × 10⁻⁷ mbar. During vapor deposition, mass spectra were recorded simultaneously to check the purity and the ratio of the deposited molecules.

The formation of ethane CH was examined by RAIR spectroscopy and TPD mass spectrometry. RAIR spectra were collected in the 4000–550 cm⁻¹ range with a spectral resolution of 2 cm⁻¹ using a Bruker Vertex 70 FT-IR spectrometer with a liquid-nitrogen-cooled mercury cadmium telluride (MCT) detector. The IR beam path outside the UHV chamber was purged with dry nitrogen gas. TPD-MS experiments were performed by a quadrupole mass spectrometer supplied by Extrel.

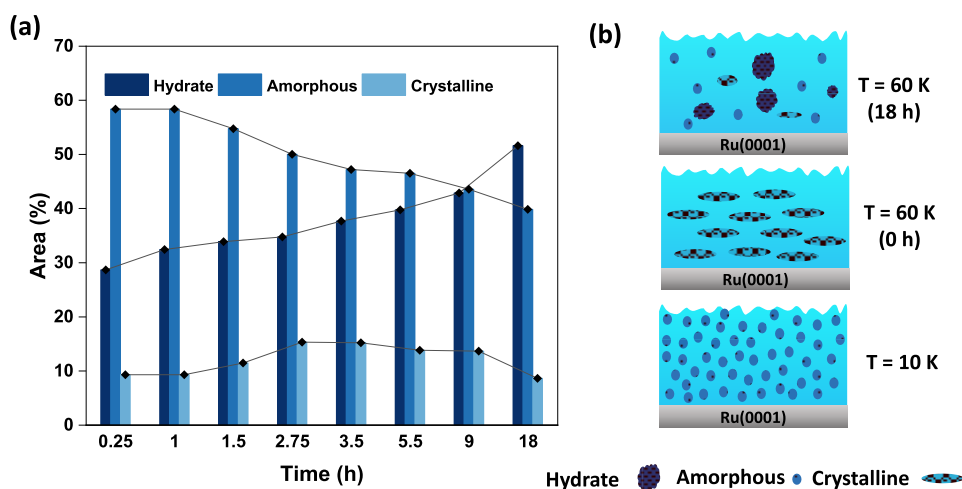


Figure 2. (a) Time-dependent growth of ethane CH. The dark blue, the blue, and the light blue bar represent ethane in hydrate, amorphous, and crystalline phases, respectively. (b) Schematic illustration of the formation of ethane hydrate, where amorphous ethane converts to crystalline ethane followed by the formation of ethane hydrate in side ice matrix.

COMPUTATIONAL DETAILS

Density functional theory (DFT) calculations were carried out to understand the effect of ethane upon inclusion in different-sized CH cages. The Gaussian 16 software was employed to perform the DFT calculations. Structural optimization and vibrational energy studies of S^{12} , $S^{12}6^2$, and $S^{12}6^4$ CH cages and ethane included S^{12} , $S^{12}6^2$, and $S^{12}6^4$ CH cages were performed at B3LYP/6-311++G(d,p) level of theory. The molecular structures of S^{12} , $S^{12}6^2$, and $S^{12}6^4$ CH cages reported by Ningru Sun et al.³⁷ were considered for the calculations. The CH cages were optimized structurally, and their vibrational modes were calculated. The optimized molecular structure of ethane was inserted into the center of the optimized CH cages, and the whole system was further optimized. The vibrational modes of the ethane inserted in CH cages were calculated. The absence of imaginary vibrational modes in the ethane inserted CH cages revealed that the optimized structures corresponded to global minima.

RESULTS AND DISCUSSION

The formation of ethane CH was studied by preparing a thin film of 300 ML ethane/ H_2O (1:1) ice mixture on Ru(0001) at 10 K. The vapor-deposited pure ethane exists in the amorphous phase at 10 K, which converts to a crystalline phase upon heating to 30 K before desorbing from the substrate at 60 K (results are shown in Figure S1a (RAIR spectra), S1b (TPD-MS data)).^{38–40} However, in ethane–water ice, ethane stays as amorphous at 10 K (full-scale RAIR spectrum showed in Figure S2) and converts to crystalline phase at 50 K. Upon further annealing to 60 K, ethane molecules desorb while leaving a fraction of ethane trapped in the ASW matrix. These trapped molecules undergo a phase evolution in the course of time.

Figure 1a shows the normalized time-dependent RAIR spectra of the ice mixture at 60 K for 0.25, 9, and 18 h in the C–H antisymmetric region of ethane, while the parent IR spectra are shown in Figure S3. The spectrum at 0.25 h (Figure 1a, blue trace) shows three distinct peaks at 2972, 2976, and 2982 cm^{-1} corresponding to the crystalline, amorphous, and CH phases, respectively. After 9 h (green trace), a slight increase in the relative intensity of the peak at 2982 cm^{-1} can

be seen, which further increased after 18 h (red trace) along with a relative decrease in the peak intensity at 2976 cm^{-1} . The assignment of the CH peak at 2982 cm^{-1} is based on the previous IR studies.^{32,41} Also, it is well-known that the vibrational frequency of a molecule entrapped in a CH cage should fall between the vibrational frequencies of the solid and gaseous phases, and the guest molecule within the CH cage behaves as a free molecule.⁴² The observed CH peak at 2982 cm^{-1} is close to the vibrational frequency of the gas phase ethane (at 2985 cm^{-1}) in the C–H antisymmetric region,⁴³ indicating the entrapment of ethane in the CH cage. The RAIR spectral peak at 2976 cm^{-1} for the amorphous phase and the peak at 2972 cm^{-1} for the crystalline phase of ethane in ethane–water ice mixture at 60 K are based on a comparison with the data of amorphous⁴⁴ and crystalline^{38,44} ethane ices (Figure S1a).

To present a clear view of the phase separation of ethane inside the ice matrix at 60 K, we have done an isothermal time-dependent RAIR study of pure ethane at 53 K (Figure S4). The intensity of the IR peak in the C–H antisymmetric region gradually decreases with the desorption of ethane from the substrate. We have not observed any peak other than the peak at 2974 cm^{-1} in pure ethane, which is attributed to the crystalline phase. Therefore, the peaks at 2976 and 2982 cm^{-1} in Figure 1b are two entirely new peaks that arise due to the formation of amorphous and CH phases inside the ice matrix. The spectrum obtained at 60 K after 18 h of annealing was deconvoluted (shown in Figure 1b) to evaluate the ratio of the three coexisting phases. Taking the area under each deconvoluted peak, the ratios of three phases, CH, amorphous and crystalline forms of ethane in the ice matrix, were estimated to be 52:40:8 by molar ratio. Although the concentration of the CH form appears to be large, it was estimated to be $\sim 2.5\%$ of the total ethane deposited.

In UHV and at cryogenic temperatures, CH formation depends on the mobility and hydrogen bonding of the host and guest molecules. Keeping the ethane–water ice mixture near the desorption temperature of ethane (60 K) is crucial for CH formation of ethane. At this temperature, higher ethane mobility leads to the formation of a clathrate-like structure in the ice matrix. We have also monitored the O–H stretching and dangling O–H region during the formation of CH. In the

O–H stretching region (Figure S5a), no significant changes were noticed, but in the dangling O–H region, the peak at 3667 cm^{-1} disappeared upon the formation of CH (Figure S5b), which suggested the collapse of micropores in ASW.^{45,46} To see the temperature dependency of CH formation, we annealed the ethane/H₂O (1:1) ice mixture at 55 K for 18 h. We did not observe any peak arising at 2982 cm^{-1} (Figure S6). Hence, we concluded that CH formation of ethane in UHV at cryogenic temperatures depends significantly on the temperature and annealing time. Figure 2a shows the time-dependent growth of ethane CH relative to the amorphous and crystalline phases. Although the overall intensity of the time-dependent RAIR spectra in the C–H antisymmetric region decreases with time, the hydrate peak intensity decreases slower relative to the amorphous peak intensity. Each RAIR spectrum in the C–H antisymmetric region at a particular time was deconvoluted into three peaks (for CH, amorphous, and crystalline phase) to estimate the area under each peak. The ratios of ethane in three phases were derived, converted into percentages, and plotted in Figure 2a. A relative increase in the fraction of the CH phase and a relative decrease in the amorphous phase was noticed, whereas the change in the fraction of the crystalline phase was roughly the same (considering the error involved in fitting). A relative increase in the fraction of the CH phase could be due to the conversion of amorphous ethane into the CH phase. The physical transformation of ethane from the amorphous to CH phase through the crystalline phase is illustrated in Figure 2b.

The formation of ethane CH in UHV was further confirmed using TPD-MS studies. Two sets of TPD-MS experiments were performed, and the results are shown in Figure 3. In the first experiment, we deposited 300 ML of ethane/H₂O (1:1) ice mixture at 10 K and heated it to 200 K with a ramping rate of 30 K min^{-1} . The desorption of ethane was monitored by $m/z = 28$ (C_2H_4^+). TPD-MS spectra were plotted as C_2H_4^+ ion intensity versus substrate temperature (blue trace). Two peaks were observed at 60 and 140 K. The peak at 60 K is attributed

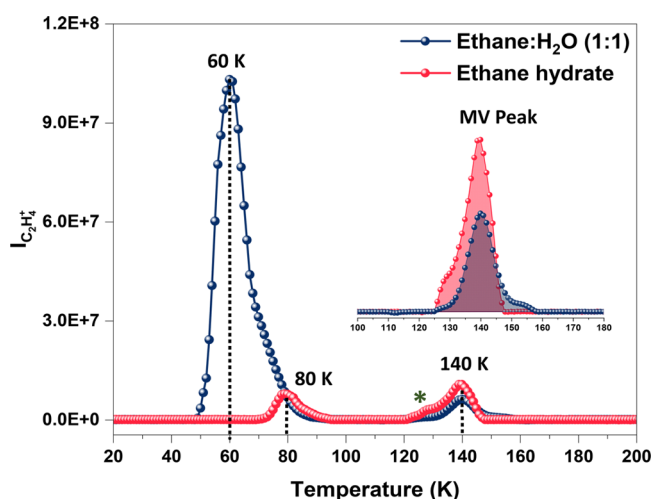


Figure 3. TPD mass spectra of 300 ML of codeposited ethane/H₂O (1:1) ice mixture (ramping rate = 30 K min^{-1}). Here, the intensity of C_2H_4^+ ($m/z = 28$) versus substrate temperature is plotted. The desorption profile of ethane after CH formation is shown with a red trace while before CH formation is shown with a blue trace. MV peak is shown in the inset. The peak labeled (*), is attributed to predissociation of ethane CH.

to the bulk desorption of ethane from ASW; the long tail of this peak is due to the molecules that are trapped in ASW pores which slowly desorbed until reaching 90 K. The peak at 140 K is attributed to the so-called molecular volcano (MV) peak.^{47,48} The MV peak occurs due to the abrupt gas release from ASW during the process of ASW crystallization. In the second experiment, we created amorphous ethane/H₂O (1:1) ice mixture at 10 K, and after annealing the sample at 60 K for 18 h (to create ethane CH), the sample was cooled to 10 K. Now, the sample was further heated to 200 at 30 K min^{-1} , and the TPD spectrum was recorded (red trace). Here, also, two peaks were observed at 80 and 140 K. The peak at 80 K is attributed to the desorption of trapped ethane (amorphous or crystalline) from the ASW matrix. The peak shift from 60 to 80 K for ethane desorption may be due to the formation of CH as well as the compactness of the ice sample (a result of prolonged annealing). In this case, the MV peak (at 140 K, red trace) shows a higher peak intensity with respect to the previous MV peak (blue trace). An increase in the intensity of MV peak for the latter case is due to the release of the trapped ethane from the ASW pores as well as due to dissociation of the CH cage. Here, it is worth noting that, in both experiments, the number of molecules of ethane and water deposited on the Ru(0001) was approximately the same. The peak marked by an asterisk around 125 K is the desorption of ethane due to the predissociation of CH cages.¹⁸

The vibrational shift in the infrared/Raman spectra upon enclathration of guest molecules inside the water cage plays a major role in understanding the types of CH structure formed.⁴⁹ Quantum chemical calculations have been used to understand the spectral properties of molecules in specific cages.⁵⁰

Particularly, DFT calculations are widely used to find the vibrational shifts in Raman and IR frequencies of methane or CH structure.⁵¹ Such studies performed at B3LYP (level of theory) are known to reproduce spectral behavior accurately.^{18,49,50} In this study, we examined different cages and the effect of entrapment of ethane in them at B3LYP/6-311++G(d,p) level of theory. We calculated the harmonic vibrational frequencies of pure ethane, empty water cages (5^{12} , $5^{12}6^2$, and $5^{12}6^4$), and ethane entrapped in three different CH cages. Figure 4 shows the optimized structures of ethane entrapped in different CH cages (5^{12} , $5^{12}6^2$, and $5^{12}6^4$). Full-scale IR spectra of ethane and ethane trapped in three cages are shown in Figure S7. The frequency shifts in the C–H antisymmetric region for free ethane and ethane engaged in 5^{12} , $5^{12}6^2$, and $5^{12}6^4$ cages are presented in Table 1. Here, positive frequency shifts were found in all three CH cages due to the dispersion interaction between the entrapped ethane and water molecules of the cage.⁵¹ A higher blue shift was found for the small cage compared to the large cages due to larger confinement, leading to the higher interaction between ethane and water. Figure 5 compares the experimental and theoretical shifts in the C–H antisymmetric stretching region. The peak shift between the deconvoluted hydrate peak and condensed ethane–water ice mixture peak at 10 K is shown in Figure 5a, whereas the peak shift between pure ethane and ethane engaged inside $5^{12}6^2$ cage is shown in Figure 5b. The experimental shift (6 cm^{-1}) closely matches the theoretical shift (7 cm^{-1}) for the $5^{12}6^2$ cage. From the above results, it was concluded that ethane forms sI CH in UHV at cryogenic temperatures.^{32,52}

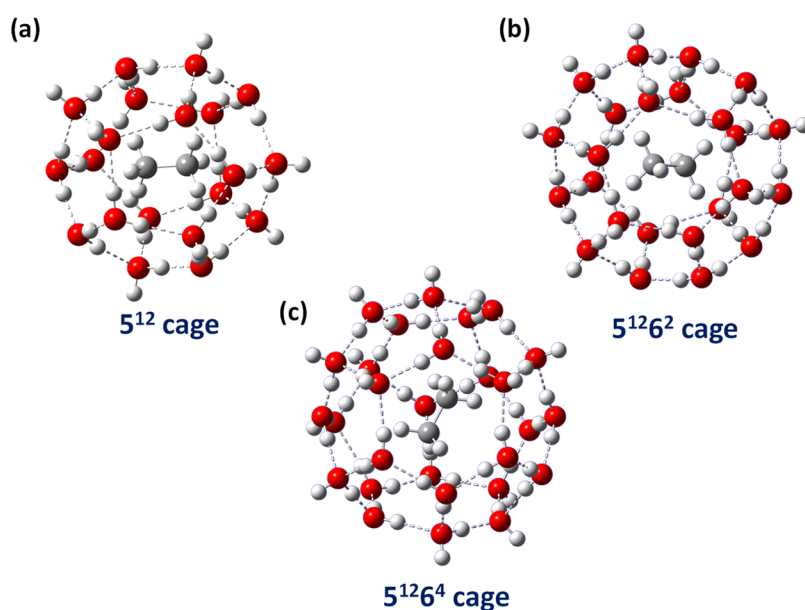


Figure 4. DFT-optimized structures of ethane trapped within different CH cages, such as (a) 5^{12} cage, (b) $5^{12}6^2$ cage, and (c) $5^{12}6^4$ cage. Here, water cage and the guest molecule ethane are shown. Color code used: gray, C atom; red, O atom; white, H atom.

Table 1. Comparison of the Computational and Experimental Vibrational Shifts of Ethane CH Compared to Free Ethane in the C–H Antisymmetric Region

ethane clathrate hydrate	5^{12} cage	$5^{12}6^2$ cage	$5^{12}6^4$ cage
Vibrational Shift (computational)	41 cm^{-1}	7 cm^{-1}	2 cm^{-1}
Vibrational Shift (Experimental)		6 cm^{-1}	

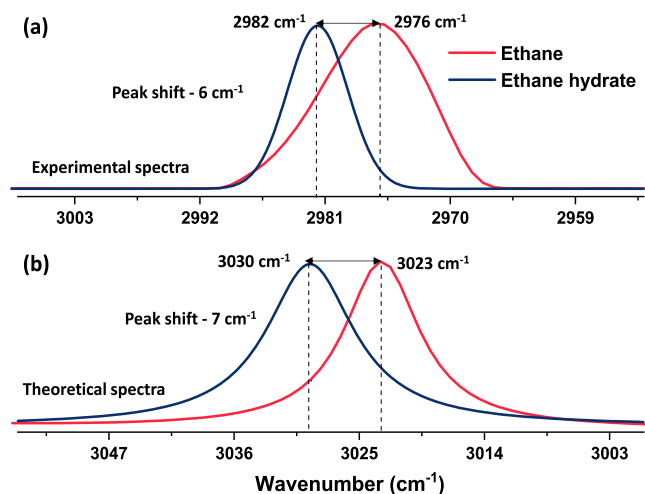


Figure 5. Comparison of experimental and theoretical IR vibrational shift in the C–H antisymmetric region of ethane due to the formation of ethane hydrate. (a) Comparison between the RAIR spectra of ethane in the ASW matrix at 10 K (red trace) and the ethane hydrate (blue trace). The hydrate peak is a deconvoluted peak from the parent RAIR spectrum collected after 18 h at 60 K in the hydrate experiment. (b) Comparison between the IR spectra of pure ethane (red trace) and ethane trapped in $5^{12}6^2$ CH cage (blue trace).

CONCLUSION

In this study, we reported the formation of ethane CH from ethane–water ice mixture at 60 K in UHV for the first time. Upon the formation of ethane CH, a 6 cm^{-1} blue shift was observed in the IR spectrum, which closely matches the

theoretical shift (7 cm^{-1}) calculated from a DFT study. Along with CH, two other ethane phases (amorphous and crystalline) also coexist in the ice mixture for a longer period at 60 K. All three phases are metastable at this temperature; therefore, upon waiting for 18 h, ethane molecules slowly desorbed from the ASW matrix. We have also discussed the evolution of three phases with respect to time and showed an approximate percentage of the distinct phases at a particular time. After waiting at 60 K for 18 h, it was seen that only 2.5% of ethane molecules stayed in the CH phase from the total deposited ethane molecules. Higher mobility of the ethane molecules near its desorption temperature leads to the formation of CH at cryogenic temperatures. RAIRS and TPD-MS were used to prove the formation of CH. Quantum chemical calculations were carried out to study the spectral behavior of ethane inside different water cages, which suggests the formation of sl CH ($5^{12}6^2$ cage) within the ice matrix. Our study gives direct evidence for the possibility of finding ethane CH in cometary environments.

ASSOCIATED CONTENT

Supporting Information

The Supporting Information is available free of charge at <https://pubs.acs.org/doi/10.1021/acs.jpcc.2c06264>.

Temperature and time-dependent RAIR spectra of pure ethane and ethane–water ice mixture, TPD-MS spectra of pure ethane and ethane–water ice mixture, theoretical IR spectra of ethane CH (PDF)

AUTHOR INFORMATION

Corresponding Author

Thalappil Pradeep – DST Unit of Nanoscience (DST UNS) and Thematic Unit of Excellence (TUE), Department of Chemistry, Indian Institute of Technology Madras, Chennai 600036, India; International Centre for Clean Water, IIT Madras Research Park, Chennai 6000113, India; orcid.org/0000-0003-3174-534X; Email: pradeep@iitm.ac.in

Authors

Bijesh K. Malla – DST Unit of Nanoscience (DST UNS) and Thematic Unit of Excellence (TUE), Department of Chemistry, Indian Institute of Technology Madras, Chennai 600036, India

Gaurav Vishwakarma – DST Unit of Nanoscience (DST UNS) and Thematic Unit of Excellence (TUE), Department of Chemistry, Indian Institute of Technology Madras, Chennai 600036, India

Soham Chowdhury – DST Unit of Nanoscience (DST UNS) and Thematic Unit of Excellence (TUE), Department of Chemistry, Indian Institute of Technology Madras, Chennai 600036, India

Premkumar Selvarajan – DST Unit of Nanoscience (DST UNS) and Thematic Unit of Excellence (TUE), Department of Chemistry, Indian Institute of Technology Madras, Chennai 600036, India

Complete contact information is available at:

<https://pubs.acs.org/10.1021/acs.jpcc.2c06264>

Author Contributions

B.K.M and G.V designed the experiments, B.K.M., G.V., and S.C performed the experiments and analyzed the results. P.S. performed the theoretical calculations. T.P. proposed the project and supervised the progress. The manuscript was written with the contributions of all authors.

Notes

The authors declare no competing financial interest.

ACKNOWLEDGMENTS

We acknowledge the Science and Engineering Research Board (SERB), Department of Science and Technology (DST), and Government of India for support. T.P. acknowledges funding from the Centre of Excellence on Molecular Materials and Functions under the Institution of Eminence scheme of IIT Madras. B.K.M. thanks the Council of Scientific and Industrial Research (CSIR) for his research fellowship. G.V. and S.C. thanks IITM for their research fellowships.

REFERENCES

- (1) Davy, H., VIII On a Combination of Oxymuriatic Gas and Oxygene Gas. *Philos. Trans. R. Soc. London* **1811**, 101, 155–162.
- (2) Chong, Z. R.; Yang, S. H. B.; Babu, P.; Linga, P.; Li, X. Sen. Review of Natural Gas Hydrates as an Energy Resource: Prospects and Challenges. *Appl. Energy* **2016**, 162, 1633–1652.
- (3) Sloan, E. D. Fundamental Principles and Applications of Natural Gas Hydrates. *Nature*; Nature Publishing Group, 2003; pp 353–359.
- (4) Yin, Z.; Zheng, J.; Kim, H.; Seo, Y.; Linga, P. Hydrates for Cold Energy Storage and Transport: A Review. *Adv. Appl. Energy* **2021**, 2, 100022.
- (5) Zheng, J.; Chong, Z. R.; Qureshi, M. F.; Linga, P. Carbon Dioxide Sequestration via Gas Hydrates: A Potential Pathway toward Decarbonization. *Energy Fuels* **2020**, 34 (9), 10529–10546.
- (6) Bhattacharjee, G.; Goh, M. N.; Arumuganainar, S. E. K.; Zhang, Y.; Linga, P. Ultra-Rapid Uptake and the Highly Stable Storage of Methane as Combustible Ice. *Energy Environ. Sci.* **2020**, 13 (12), 4946–4961.
- (7) Thomas, C.; Mousis, O.; Picaud, S.; Ballenegger, V. Variability of the Methane Trapping in Martian Subsurface Clathrate Hydrates. *Planet. Space Sci.* **2009**, 57 (1), 42–47.
- (8) Chastain, B. K.; Chevrier, V. Methane Clathrate Hydrates as a Potential Source for Martian Atmospheric Methane. *Planet. Space Sci.* **2007**, 55 (10), 1246–1256.
- (9) Tobie, G.; Lunine, J. I.; Sotin, C. Episodic Outgassing as the Origin of Atmospheric Methane on Titan. *Nature* **2006**, 440 (7080), 61–64.
- (10) Mousis, O.; Lunine, J. I.; Picaud, S.; Cordier, D. Volatile Inventories in Clathrate Hydrates Formed in the Primordial Nebula. *Faraday Discuss.* **2010**, 147 (0), 509–525.
- (11) Cui, J.; Sun, Z.; Wang, X.; Yu, B.; Leng, S.; Chen, G.; Sun, C. Fundamental Mechanisms and Phenomena of Clathrate Hydrate Nucleation. *Chin. J. Chem. Eng.* **2019**, 27 (9), 2014–2025.
- (12) Englezos, P. *REVIEWS Clathrate Hydrates* **1993**.
- (13) Truong-Lam, H. S.; Seo, S.; Kim, S.; Seo, Y.; Lee, J. D. In Situ Raman Study of the Formation and Dissociation Kinetics of Methane and Methane/Propane Hydrates. *Energy Fuels* **2020**, 34 (5), 6288–6297.
- (14) Nagashima, H. D.; Ohmura, R. Phase Equilibrium Condition Measurements in Methane Clathrate Hydrate Forming System from 197.3 to 238.7 K. *J. Chem. Thermodyn* **2016**, 102, 252–256.
- (15) Fleyfel, F.; Devlin, J. P. FT-IR Spectra of 90 K Films of Simple, Mixed, and Double Clathrate Hydrates of Trimethylene Oxide, Methyl Chloride, Carbon Dioxide, Tetrahydrofuran, and Ethylene Oxide Containing Decoupled D2O. *J. Phys. Chem.* **1988**, 92, 631–635.
- (16) Blake, D.; Allamandola, L.; Sandford, S.; Hudgins, D.; Freund, F. Clathrate Hydrate Formation in Amorphous Cometary Ice Analogs in Vacuo. *Science (80-)* **1991**, 254 (5031), 548–551.
- (17) Bauer, R. P. C.; Ravichandran, A.; Tse, J. S.; Appathurai, N.; King, G.; Moreno, B.; Desgreniers, S.; Sammynaiken, R. In Situ X-Ray Diffraction Study on Hydrate Formation at Low Temperature in a High Vacuum. *J. Phys. Chem. C* **2021**, 125 (48), 26892–26900.
- (18) Ghosh, J.; Methikkalam, R. R. J.; Bhuin, R. G.; Ragupathy, G.; Choudhary, N.; Kumar, R.; Pradeep, T. Clathrate Hydrates in Interstellar Environment. *Proc. Natl. Acad. Sci. U. S. A* **2019**, 116 (5), 1526–1531.
- (19) Murshed, M. M.; Schmidt, B. C.; Kuhs, W. F. Kinetics of Methane-Ethane Gas Replacement in Clathrate-Hydrates Studied by Time-Resolved Neutron Diffraction and Raman Spectroscopy. *J. Phys. Chem. A* **2010**, 114 (1), 247–255.
- (20) Thakre, N.; Jana, A. K. Physical and Molecular Insights to Clathrate Hydrate Thermodynamics. *Renew. Sustain. Energy Rev.* **2021**, 135, 110150.
- (21) Ghosh, J.; Bhuin, R. G.; Vishwakarma, G.; Pradeep, T. Formation of Cubic Ice via Clathrate Hydrate, Prepared in Ultrahigh Vacuum under Cryogenic Conditions. *J. Phys. Chem. Lett.* **2020**, 11 (1), 26–32.
- (22) Ghosh, J.; Bhuin, R. G.; Ragupathy, G.; Pradeep, T. Spontaneous Formation of Tetrahydrofuran Hydrate in Ultrahigh Vacuum. *J. Phys. Chem. C* **2019**, 123 (26), 16300–16307.
- (23) Cwiklik, L.; Devlin, J. P. Hindering of Rotational Motion of Guest Molecules in the Type I Clathrate Hydrate. *Chem. Phys. Lett.* **2010**, 494 (4–6), 206–212.
- (24) Fleyfel, F.; Devlin, J. P. FT-IR Spectra of 90 K Films of Simple, Mixed, and Double Clathrate Hydrates of Trimethylene Oxide, Methyl Chloride, Carbon Dioxide, Tetrahydrofuran, and Ethylene Oxide Containing Decoupled D2O. *J. Phys. Chem.* **1988**, 92 (3), 631–635.
- (25) Egelman, E. H. Cryo-EM: Ice Is Nice, but Good Ice Can Be Hard to Find. *Biophys. J.* **2020**, 118 (6), 1238.
- (26) Ghosh, J.; Vishwakarma, G.; Das, S.; Pradeep, T. Facile Crystallization of Ice Ih via Formaldehyde Hydrate in Ultrahigh Vacuum under Cryogenic Conditions. *J. Phys. Chem. C* **2021**, 125 (8), 4532–4539.
- (27) Falenty, A.; Hansen, T. C.; Kuhs, W. F. Formation and Properties of Ice XVI Obtained by Emptying a Type II Clathrate Hydrate. *Nature* **2014**, 516 (7530), 231–233.
- (28) Horowitz, Y.; Asscher, M. Electron-Induced Chemistry of Methyl Chloride Caged within Amorphous Solid Water. *J. Chem. Phys.* **2013**, 139 (15), 154707.
- (29) Van Dishoeck, E. F.; Herbst, E.; Neufeld, D. A. Interstellar Water Chemistry: From Laboratory to Observations. *Chemical Reviews* **2013**, 113, 9043–9085.

- (30) Öberg, K. I. Photochemistry and Astrochemistry: Photochemical Pathways to Interstellar Complex Organic Molecules. *Chem. Rev.* **2016**, *116* (17), 9631–9663.
- (31) Singh, S. K.; Zhu, C.; La Jeunesse, J.; Fortenberry, R. C.; Kaiser, R. I. Experimental Identification of Aminomethanol (NH₂CH₂OH)—the Key Intermediate in the Strecker Synthesis. *Nat. Commun.* **2022**, *13* (1), 1–7.
- (32) Richardson, H. H.; Wooldridge, P. J.; Devlin, J. P. FT-IR Spectra of Vacuum Deposited Clathrate Hydrates of Oxirane H₂S, THF, and Ethane. *J. Chem. Phys.* **1985**, *83* (9), 4387.
- (33) Mumma, M. J.; DiSanti, M. A.; Dello Russo, N.; Fomenkova, M.; Magee-Sauer, K.; Kaminski, C. D.; Xie, D. X. Detection of Abundant Ethane and Methane, along with Carbon Monoxide and Water, in Comet C/1996 B2 Hyakutake: Evidence for Interstellar Origin. *Science* (80-.) **1996**, *272* (5266), 1310–1314.
- (34) Dello Russo, N.; Mumma, M. J.; DiSanti, M. A.; Magee-Sauer, K. Production of Ethane and Water in Comet C/1996 B2 Hyakutake. *J. Geophys. Res. Planets* **2002**, *107* (E11), 5-1–5-11.
- (35) Bag, S.; Bhuin, R. G.; Methikkalam, R. R. J.; Pradeep, T.; Kephart, L.; Walker, J.; Kuchta, K.; Martin, D.; Wei, J. Development of Ultralow Energy (1–10 eV) Ion Scattering Spectrometry Coupled with Reflection Absorption Infrared Spectroscopy and Temperature Programmed Desorption for the Investigation of Molecular Solids. *Rev. Sci. Instrum.* **2014**, *85* (1), 014103.
- (36) Kim, Y.; Moon, E.; Shin, S.; Kang, H. Acidic Water Monolayer on Ruthenium(0001). *Angew. Chem.* **2012**, *124* (51), 12978–12981.
- (37) Sun, N.; Li, Z.; Qiu, N.; Yu, X.; Zhang, X.; Li, Y.; Yang, L.; Luo, K.; Huang, Q.; Du, S. Ab Initio Studies on the Clathrate Hydrates of Some Nitrogen- and Sulfur-Containing Gases. *J. Phys. Chem. A* **2017**, *121* (13), 2620–2626.
- (38) Tejada, S. B.; Eggers, D. F. Infrared Spectra of Ordered Crystalline Ethane and Ethane-D₆. *Spectrochim. Acta Part A Mol. Spectrosc.* **1976**, *32* (9), 1557–1562.
- (39) Chesters, M. A.; Gardner, P.; McCash, E. M. The Reflection-Absorption Infrared Spectra of n-Alkanes Adsorbed on Pt(111). *Surf. Sci.* **1989**, *209* (1–2), 89–99.
- (40) Hudson, R. L.; Gerakines, P. A.; Moore, M. H. Infrared Spectra and Optical Constants of Astronomical Ices: II. Ethane and Ethylene. *Icarus* **2014**, *243*, 148–157.
- (41) Dartois, E.; Langlet, F. Ethane Clathrate Hydrate Infrared Signatures for Solar System Remote Sensing. *Icarus* **2021**, *357*, 114255.
- (42) Buch, V.; Devlin, J. P.; Monreal, I. A.; Jagoda-Cwiklik, B.; Uras-Aytemiz, N.; Cwiklik, L. Clathrate Hydrates with Hydrogen-Bonding Guests. *Phys. Chem. Chem. Phys.* **2009**, *11* (44), 10245–10265.
- (43) Hepp, M.; Herman, M. Weak Combination Bands in the 3-Mm Region of Ethane. *J. Mol. Spectrosc.* **1999**, *197* (1), 56–63.
- (44) Hudson, R. L.; Moore, M. H.; Raines, L. L. Ethane Ices in the Outer Solar System: Spectroscopy and Chemistry. *Icarus* **2009**, *203* (2), 677–680.
- (45) Maté, B.; Satorre, M.; Escribano, R. On the Spectral Features of Dangling Bonds in CH₄/H₂O Amorphous Ice Mixtures. *Phys. Chem. Chem. Phys.* **2021**, *23* (15), 9532–9538.
- (46) Li, H.; Karina, A.; Ladd-Parada, M.; Späh, A.; Perakis, F.; Benmore, C.; Amann-Winkel, K. Long-Range Structures of Amorphous Solid Water. *J. Phys. Chem. B* **2021**, *125* (48), 13320–13328.
- (47) Collings, M. P.; Anderson, M. A.; Chen, R.; Dever, J. W.; Viti, S.; Williams, D. A.; McCoustra, M. R. S. A Laboratory Survey of the Thermal Desorption of Astrophysically Relevant Molecules. *Mon. Not. R. Astron. Soc.* **2004**, *353*, 1133–1140, DOI: 10.1111/j.1365-2966.2004.08272.x.
- (48) May, R. A.; Smith, R. S.; Kay, B. D. The Release of Trapped Gases from Amorphous Solid Water Films. I. “Top-down” Crystallization-Induced Crack Propagation Probed Using the Molecular Volcano. *J. Chem. Phys.* **2013**, *138* (10), 104501.
- (49) Ghosh, J.; Bhuin, R. G.; Ragupathy, G.; Pradeep, T. Spontaneous Formation of Tetrahydrofuran Hydrate in Ultrahigh Vacuum. *J. Phys. Chem. C* **2019**, *123* (26), 16300–16307.
- (50) Li, M.; Li, K.; Yang, L.; Su, Y.; Zhao, J.; Song, Y. Evidence of Guest-Guest Interaction in Clathrates Based on in Situ Raman Spectroscopy and Density Functional Theory. *J. Phys. Chem. Lett.* **2022**, *13* (1), 400–405.
- (51) Ramya, K. R.; Pavan Kumar, G. V.; Venkatnathan, A. Raman Spectra of Vibrational and Librational Modes in Methane Clathrate Hydrates Using Density Functional Theory. *J. Chem. Phys.* **2012**, *136* (17), 174305.
- (52) Hoshikawa, A. Structural Changes Due to the Ordered Guest Molecules in Deuterated Ethane Hydrate. *Chem. Phys. Lett.* **2022**, *800*, 139679.

Recommended by ACS

Phase Behavior of Clathrate Hydrates in the Ternary H₂O–NH₃–Cyclopentane System

Claire Petuya, Ashley G. Davies, *et al.*

MARCH 23, 2020
ACS EARTH AND SPACE CHEMISTRY

READ 

CH/CH₂ Group Clusters Doping Methane Hydrate Cages

Lihua Wan, Shuanshi Fan, *et al.*

OCTOBER 20, 2022
THE JOURNAL OF PHYSICAL CHEMISTRY LETTERS

READ 

Hydrate Stability in the H₂S–H₂O system—Visual Observations and Measurements in a High-Pressure Optical Cell and Thermodynamic Models

Jiyue Sun, Lei Jiang, *et al.*

JUNE 30, 2020
JOURNAL OF CHEMICAL & ENGINEERING DATA

READ 

Structural Transition of the Methane–Ethane Mixture Hydrate in a Hydrate/Water/Hydrocarbon Three-Phase Coexistence System: Effect of Gas Concentration

Jiangtao Pang, Satoshi Takeya, *et al.*

NOVEMBER 03, 2020
ACS SUSTAINABLE CHEMISTRY & ENGINEERING

READ 

Get More Suggestions >